# Self-Assembly of Gold(I) Rings and Reversible Formation of Organometallic [2]Catenanes

**Christopher P. McArdle,[a] Michael J. Irwin,[a] Michael C. Jennings,[a] Jagadese J. Vittal,[b] and Richard J. Puddephatt*[a]**

**Abstract:** The reaction of the digold(I) diacetylide $[(AuCCCH_2OC_6H_4)_2CMe_2]$ with diphosphane ligands can lead to formation of either macrocyclic ring complexes or [2]catenanes by self-assembly. This gives an easy route to rare organometallic [2]catenanes, and the effect of the diphosphane ligand on the selectivity of self-assembly is studied. With diphosphane ligands $Ph_2P(CH_2)_xPPh_2$, the simple ring complex $[Au_2\{(CCCH_2OC_6H_4)_2CMe_2\}(Ph_2P(CH_2)_xPPh_2)]$ is formed selectively when $x = 2$, but the [2]catenanes $[Au_2\{(CCCH_2OC_6H_4)_2CMe_2\}(Ph_2P(CH_2)_xPPh_2)]_2$ are formed when $x = 4$ or 5. When $x = 3$, a mixture of the simple ring and [2]catenane is formed, along with the "double-ring" complex, $[Au_4\{(CCCH_2OC_6H_4)_2CMe_2\}_2(Ph_2P(CH_2)_3PPh_2)_2]$ and a "hexamer" $[\{Au_2[(CCCH_2OC_6H_4)_2CMe_2](Ph_2P(CH_2)_3PPh_2)\}_6]$ whose structure is not determined. A study of the equilibria between these complexes by solution NMR techniques gives insight into the energetics and mechanism of [2]catenane formation. When the oligomer $[(AuCCCH_2OC_6H_4)_2CMe_2]$ was treated with a mixture of two diphosphane ligands, or when two [2]catenane complexes $[\{Au_2[(CCCH_2OC_6H_4)_2CMe_2](diphosphane)\}_2]$ were allowed to equilibrate, only the symmetrical [2]catenanes were formed. The diphosphanes $Ph_2PCCPPh_2$, *trans*-$[Ph_2PCH{=}CHPPh_2]$ and $(Ph_2PC_5H_4)_2Fe$ give the corresponding ring complexes $[Au_2\{(CCCH_2OC_6H_4)_2CMe_2\}(diphosphane)]$, and the chiral, unsymmetrical diacetylide $[Au_2\{(CCCH_2OC_6H_4C(Me)(CH_2CMe_2)C_6H_3OCH_2CC)]$ gives macrocyclic ring complexes with all diphosphane ligands $Ph_2P(CH_2)_xPPh_2$ ($x = 2-5$).

**Keywords:** aurophilicity · catenanes · gold · molecular recognition · self-assembly

## Introduction

There is considerable interest in the development of supramolecular systems which may have application in nanoscale devices, and the prospects of success have increased as a result of recent advances in the synthesis of mechanically interlocked molecules.[1–3] By far the most explored and understood area of this work has been the study of [2]catenanes, and a large number of synthetic strategies based on ideas such as $\pi-\pi$ interactions, cation templation, hydrophobic forces, and hydrogen bonding have been developed.[4] Most advances have used the techniques of organic and coordination chemistry, or combinations of both, but the field of organometallic catenanes is still in its infancy.[5] The first examples of catenanes containing organometallic centers were the organomagnesium compound **A**,[6] with metal in one ring only, and the σ,π-bonded gold(I) acetylide complex **B** (R = *t*Bu).[7] For different reasons, neither synthetic method can be easily applied to the synthesis of other catenane complexes, and a rational synthetic procedure is a prerequisite for systematic studies.

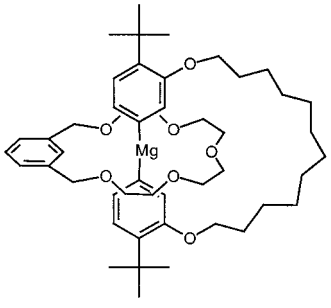


**A**

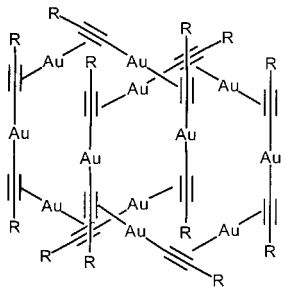


**B**

Recent research on the synthesis of linear-chain metal-containing polymers with extended backbone conjugation through $d\pi-p\pi$ hybridization,[8] as required for applications in advanced materials,[9] has focussed on gold(I) chemistry

[a] Prof. R. J. Puddephatt, Dr. C. P. McArdle, Dr. M. J. Irwin, Dr. M. C. Jennings
Department of Chemistry
University of Western Ontario
London, ON N6A 5B7 (Canada)
Fax: (+1) 661-3022
E-mail: pudd@uwo.ca

[b] Prof. J. J. Vittal
Department of Chemistry
National University of Singapore
3 Science Drive, Singapore 117543 (Singapore)

  0947-6539/02/0803-0723 $ 17.50+.50/0 

(**C**–**E**). Gold(I) is interesting because it usually forms simple two-coordinate linear complexes[10] and it has the potential to orient chains through aurophilic attractions (shown as Au···Au, with typical distances of 2.75–3.40 Å and bond energies of 7–11 kcal mol$^{-1}$).[11] During the course of this research, the first organometallic system that is predisposed to spontaneous formation of catenated molecular structures was discovered.[12, 13]

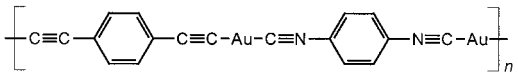


**C**

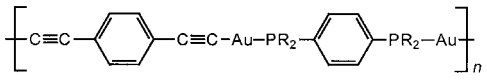


**D**

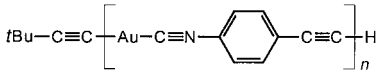


**E**

Herein we describe how reaction of a flexible dialkynyl digold(I) complex with diphosphane ligands can yield either macrocyclic or [2]catenane products in high yields, and it is shown that the outcome of the self-assembly reaction is dependent upon the nature of the spacer group in the diphosphane ligand. The spectroscopic, structural, and photophysical data of these new macrocyclic complexes are discussed in detail, along with attempts to synthesize both mixed-ligand catenanes and chiral catenanes. A preliminary report of some of these findings has been published,[12] and a study of how conformational effects of the diacetylide ligand can influence [2]catenane formation has been reported.[13]

## Results and Discussion

**Ligand and gold(I) oligomer synthesis**: Reaction of 4,4′-isopropylidenebisphenol (**1**) with propargyl bromide under basic conditions gave the bis(alkyne) derivative **2**, which was easily converted to the oligomeric digold(I) diacetylide derivative **3** by reaction with [AuCl(SMe$_2$)] in the presence of sodium acetate (Scheme 1). Complex **3** was isolated, in essentially quantitative yield, as a yellow powder which was insoluble in common organic solvents. Like other gold(I) acetylides, it is presumed to have a polymeric structure in which each acetylide group is σ-bonded ($\eta^1$) to one gold atom and π-bonded ($\eta^2$) to another.[7] This is supported by the IR spectrum of **3**, which exhibits a weak band at 2000 cm$^{-1}$, considerably lower (ca. 120 cm$^{-1}$) than the corresponding band in the precursor **2** as expected if the alkynyl groups act as π donors.

**Reactions with diphosphane ligands**: Reactions of complex **3** with a variety of diphosphane ligands gave air-stable soluble cyclic gold(I) complexes (Scheme 2) in high yields. The new diphosphane complexes were characterized by elemental

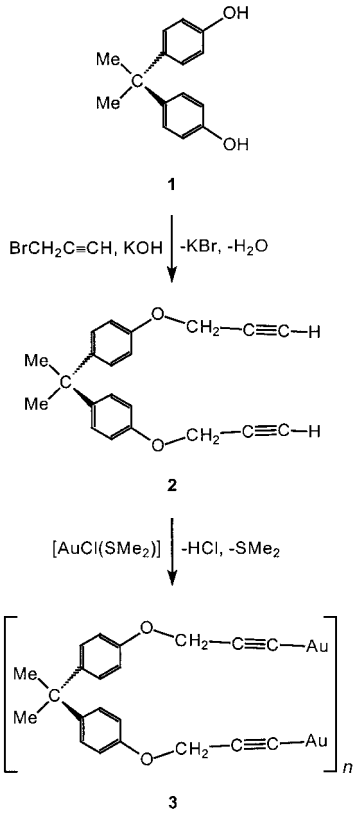


Scheme 1. Synthesis of the digold(I) diacetylide precursor **3**.

analysis, multi-nuclei NMR (both 1D and 2D), IR spectroscopy. and in a number of cases by X-ray structure determinations.

The $^{31}$P NMR spectra of the complexes showed that in all cases, except the one in which the diphosphane was bis(diphenylphosphanyl)propane (dppp), the reactions occurred selectively to give a single product. Reactions involving diphosphanes with short and/or bulky spacer groups connecting the two diphenylphosphane donor groups ($CH_2CH_2$, CC, *trans*-CH=CH, Fe($C_5H_4$)$_2$) yielded simple ring complexes (**4a, 4c**–**e**), the result of 1:1 self-assembly between the gold(I) oligomer and diphosphane. With the longer spacer groups [$(CH_2)_4$ or $(CH_2)_5$] the only products were the [2]catenane complexes **5b**–**c**, resulting from the self-assembly of two gold(I) oligomer units and two diphosphane ligands. The reaction with dppp gave a complex equilibrium of products as evidenced by the observation of four resonance siganls in the $^{31}$P NMR spectrum of the initially formed product. The $(CH_2)_3$ spacer group is thus at the transition point of the self-assembly process: shorter, bulkier linker groups give simple ring complexes **4**, while longer linker groups give the [2]catenane derivatives **5**. With dppp both **4** and **5** are identified along with two other "isomers" whose structural characterization is discussed below.

The $^1$H and $^{13}$C NMR data for all the new macrocycles were fully assigned by the use of 2D NMR techniques, and are detailed in the Experimental Section. However, whilst the NMR and IR data are in agreement with the proposed structures, they cannot distinguish between simple ring and [2]catenane structures. Low-temperature NMR studies ($^1$H



0947-6539/02/0803-0724 $ 17.50+.50/0 *Chem. Eur. J.* **2002**, *8*, No. 3

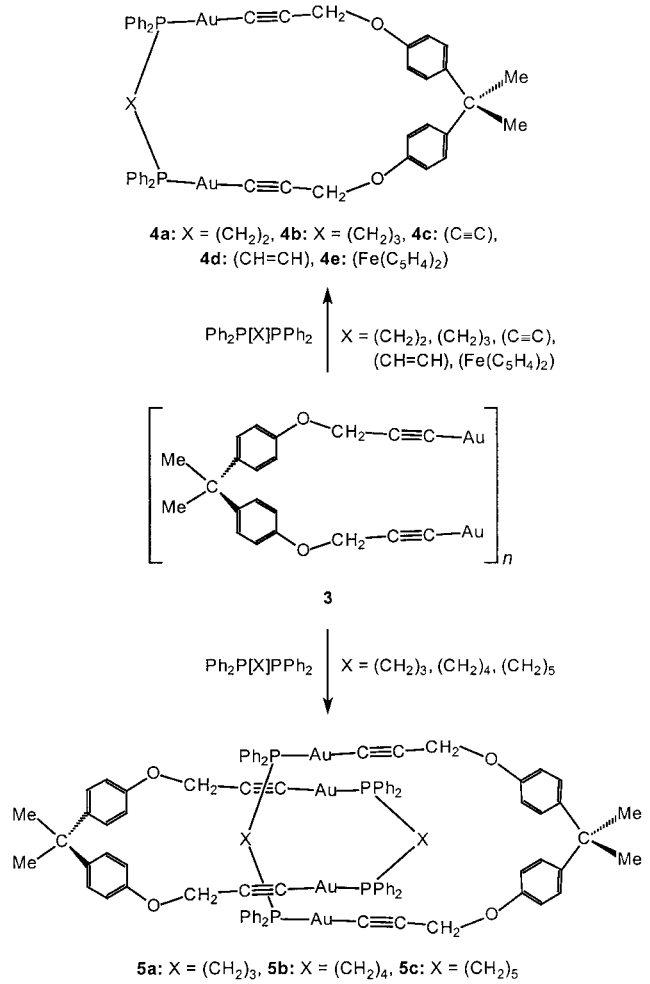


Scheme 2. Synthesis of gold rings **4** and catenanes **5**.

and $^{31}P$) did not lead to any significant changes in the spectra of **4** or **5**, indicating that any conformational asymmetry is lost by rapid intramolecular motions.[14] In principle, mass spectrometry can be used to distinguish between **4** and **5** on the basis of mass, but the technique is not fully reliable due to the ease of cleavage of the mechanical link in **5**. Preliminary studies using electron impact (EI), chemical ionization (CI), fast-atom bombardment (FAB) on solid samples or electrospray ionization (ESI) MS on solutions were unsuccessful, but matrix-assisted laser desorption ionization time-of-flight (MALDI-TOF) MS proved useful. Using this technique, the catenane **5a** gave a parent ion (*P*) at *m/z* 2218 (10%, *P*), as well as at 1109 (90%, 0.5*P*) due to fragmentation to the simple ring. The most intense peak was at *m/z* 1305 (100%, 0.5*P* + Au), corresponding to the simple ring plus one gold atom. Other significant peaks were at *m/z* 2111 (10%, $P - C_6H_4OCH_2$) and 1915 (25%, $P - Me_2C(C_6H_4OCH_2CC)_2$. A very weak molecular ion peak was observed for the larger catenane **5b** (mass $P = 2246$), but there were significant peaks at *m/z* 2140 (20%, $P - C_6H_4OCH_2$), 1943 (25%, $P$ – diacetylide), 1319 (90%, 0.5*P* + Au) and 1123 (100%, 0.5*P*), and the presence of the high mass peaks can be taken as confirmation of the [2]catenane structure. The simple ring complex **4a** gave *m/z* 1095 (100%, *P*) but also gave a peak at *m/z* 1292 (70%, *P* + Au). This (ring + Au) peak is observed for both the simple ring complexes and the [2]catenanes, so it is not a useful indicator of structure.

Interestingly, use of an excess of diphosphane ligand in reactions with the shorter spacer groups ($C_2$ and $C_3$; i.e. simple ring-forming ligands) resulted in the formation of insoluble white solid products only, which are presumably polymeric in nature. The product isolated from reaction of **3** and excess bis(diphenylphosphanyl)ethane (dppe) was shown by elemental analysis to have the stoichiometry $[Au_2\{(CCCH_2OC_6H_4)_2CMe_2\}(Ph_2P(CH_2)_2PPh_2)_2]$, corresponding to the incorporation of one unit of digold(I) diacetylide and two units of dppe. However, reactions using excess diphosphane with larger spacer groups ($C_4$ and $C_5$) yielded only the expected [2]catenane products.

**Structural characterization**: X-ray structure determinations were carried out for five of the macrocyclic products, three simple rings **4a**, **4c**, and **4d**, and two [2]catenanes (**5a** and **5b**). No suitable single crystals could be obtained for the other new products. The structure of **5b** has been described previously.[15]

The molecular structure of the simple ring **4a** is shown in Figure 1, and selected bond lengths and angles are presented in Table 1. The 23-membered ring, formed from one digold(I)

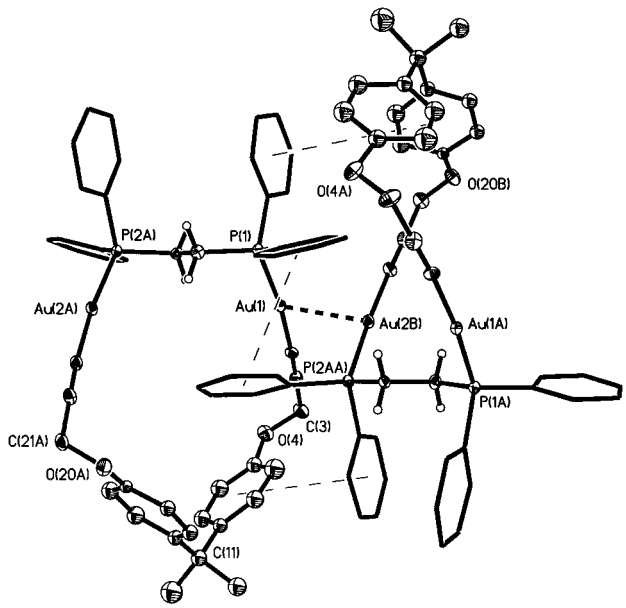


Figure 1. Structure of complex **4a** showing interactions between two adjacent molecules. Dotted lines indicate significant Au ··· Au or aryl ··· aryl secondary bonding interactions. Note the twisted conformation of the macrocyclic rings and the roughly orthogonal orientation of neighboring rings.

Table 1. Selected bond lengths [Å] and bond angles [°] for complex **4a**.

| | | | |
|---|---|---|---|
| Au(1)–P(1) | 2.277(3) | Au(2)–P(2) | 2.280(3) |
| Au(1)–C(1) | 1.97(1) | Au(2)–C(23) | 1.99(1) |
| C(1)–C(2) | 1.18(2) | C(23)–C(22) | 1.16(2) |
| C(2)–C(3) | 1.50(2) | C(22)–C(21) | 1.51(2) |
| C(1M)-P(1)-Au(1) | 109.2(4) | C(2M)-P(2)-Au(2) | 108.4(4) |
| P(1)-Au(1)-C(1) | 173.0(5) | P(2)-Au(2)-C(23) | 173.7(4) |
| Au(1)-C(1)-C(2) | 176(1) | Au(2)-C(23)-C(22) | 176(1) |
| C(1)-C(2)-C(3) | 179(2) | C(23)-C(22)-C(21) | 179(2) |
| C(10)-C(11)-C(14) | 114(3) | C(12)-C(11)-C(13) | 98(4) |

diacetylide unit and one dppe ligand, adopts an extended cyclopentane half-chair conformation, mapped by (C(11)-C(21A)-P(2A)-P(1)-C(3)). The ring is strongly puckered, with a twist angle of 60°—the two phosphorus atoms are displaced either side of the plane defined by the other atoms. This distortion from planarity is clearly a result of the need to bring the two gold atoms close enough together that they can be bridged by the diphosphane ligand. The bonding within the ring is unremarkable for this type of macrocycle, but the extended packing within the crystal lattice is particularly interesting, with a polymeric structure resulting from intermolecular interactions between adjacent molecules. As shown in Figure 1, neighboring simple rings adopt a highly efficient *anti* packing arrangement that both minimizes steric repulsions and maximizes intermolecular attractions. Adjacent molecules are held together by both a short Au···Au aurophilic attraction (Au(1)–Au(2B) 2.9668(8) Å),[11] and also by three aryl–aryl interactions (two aryl–phenyl edge-to-face (*ef*), and one phenyl-phenyl offset-face-to-face (*off*)].[16] This synergistic combination of attractive forces (typical aryl–aryl attractions have energies of about 6 kJ mol$^{-1}$, compared to 7–11 kJ mol$^{-1}$ for Au···Au interactions), must clearly lend a considerable degree of stabilization to the polymeric array.

The molecular structures of complexes **4c** and **4d** are shown in Figure 2 and Figure 3, and selected bond lengths and angles are summarized in Table 2 and Table 3, respectively. Both simple rings are isostructural to **4a**, adopting extended cyclopentane half-chair conformations and exhibiting the same polymeric crystal packing array (**4c**: Au···Au 2.9987(13) Å; **4d**: Au···Au 2.9961(11) Å]. It was expected that use of the more rigid $C_2$ ligands, bis(diphenylphosphanyl)-acetylene (dppa) and *trans*-1,2-bis(diphenylphosphanyl)ethylene (dpp$^t$e), would lead to formation of large double-rings (two digold diacetylide + two diphosphane), but this was not observed. In fact, comparison of the product macrocycles shows that with increasing ligand rigidity the puckering in the ring structure is reduced. The dppa product **4c** has the smallest twist angle (53°) and the longest P···P intramolecular nonbonding distance, 4.695 Å (c.f. **4a**: 4.423 Å; **4d**: 4.478 Å), of the three simple rings. The reduced puckering, indicates less ring flexibility and so probably increased ring strain compared to **4a**. The increased strain is evidently not sufficient to cause a different form of self-assembly to occur.

Table 2. Selected bond lengths [Å] and bond angles [°] for complex **4c**.

| | | | |
|---|---|---|---|
| Au(1)–P(1) | 2.267(5) | Au(2)–P(2) | 2.274(6) |
| Au(1)–C(7) | 2.03(3) | Au(2)–C(1) | 1.90(4) |
| C(7)–C(8) | 1.14(3) | C(1)–C(2) | 1.24(4) |
| C(11)-P(1)-Au(1) | 105.0(7) | C(10)-P(2)-Au(2) | 103.0(8) |
| P(1)-Au(1)-C(7) | 170.2(7) | P(2)-Au(2)-C(1) | 171.7(8) |
| Au(1)-C(7)-C(8) | 178(2) | Au(2)-C(1)-C(2) | 179(3) |
| C(7)-C(8)-C(9) | 175(3) | C(1)-C(2)-C(3) | 176(3) |

Table 3. Selected bond lengths [Å] and bond angles [°] for complex **4d**.

| | | | |
|---|---|---|---|
| Au(1)–P(1) | 2.274(5) | Au(2A)–P(2A) | 2.277(5) |
| Au(1)–C(11) | 2.05(2) | Au(2A)–C(21A) | 1.99(2) |
| C(11)–C(12) | 1.15(3) | C(21A)–C(22A) | 1.19(2) |
| C(1)-P(1)-Au(1) | 105.8(5) | C(2A)-P(2A)-Au(2A) | 112.1(7) |
| P(1)-Au(1)-C(11) | 170.7(6) | P(2A)-Au(2A)-C(21A) | 175.3(6) |
| Au(1)-C(11)-C(12) | 175(2) | Au(2A)-C(21A)-C(22A) | 175.6(19) |
| C(11)-C(12)-C(13) | 178(3) | C(21A)-C(22A)-C(23A) | 177(2) |

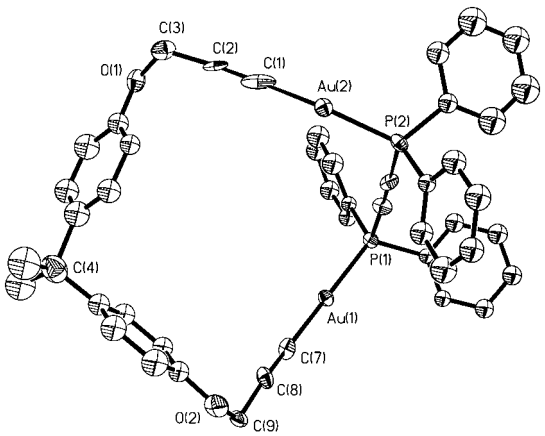


Figure 2. The macrocyclic ring structure of complex **4c**.

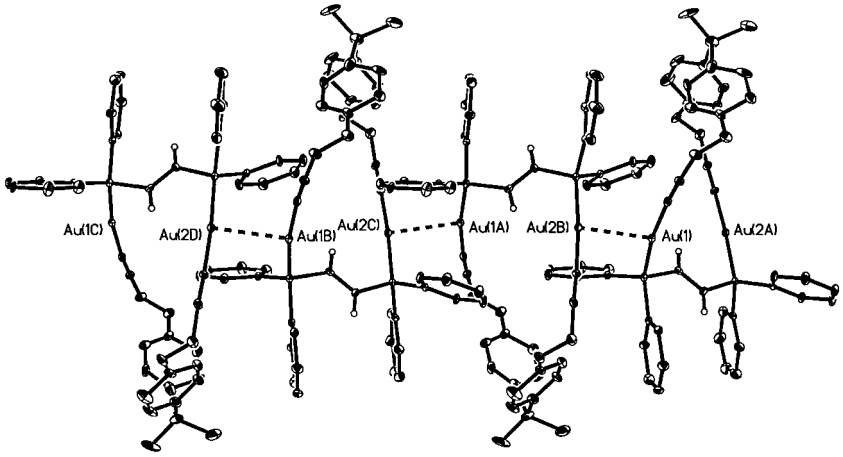


Figure 3. The chain structure formed by intermolecular aurophilic attractions between gold(I) centers of complex **4d**. Note that the rings are much less twisted than for **4a**.

In all three simple rings the bonding is similar, with regular tetrahedral geometry at the hinge carbon ($CMe_2$) atoms, and approximately linear arrangement of the P–Au–C≡C–C units. For complexes **4a** and **4c**, the bonding within the ring is essentially symmetric, about a $C_2$ axis through the hinge carbon atom and the center of the diphosphane ligand, but there is a notable distortion in complex **4d**. The angle C(1)-P(1)-Au(1) 105.8(5)°, but C(2A)-P(2A)-Au(2A) 112.1(7)°, and similarly P(1)-Au(1)-C(11) 170.7(6)°, while P(2A)-Au(2A)-C(21A) 175.3(6)°. Clearly there is a significant distortion due to ring strain. All three rings, however, must have flexibility in the solution state, undergoing rapid ring inversion, since NMR data are consistent with $C_{2v}$ symme-



0947-6539/02/0803-0726 $ 17.50+.50/0 *Chem. Eur. J.* **2002**, *8*, No. 3

try. For example, equivalence of the $OCH_2$ protons is observed in the $^1H$ NMR spectrum of all three macrocycles.

The molecular structure of the [2]catenane **5a** is shown in Figure 4, and selected bond lengths and angles are given in Table 4. The large unit cell of **5a** contains two inequivalent [2]catenanes (see Figure 4a and 4b), both formed by the self-assembly of two digold(I) diacetylide units and two diphosphane ligands. Each catenane exists as two 24-membered rings that interlock symmetrically across the methylene chain of the diphosphane ligands. The individual components are similar to the simple rings, **4a**, **4c**, and **4d**, adopting pseudocyclopentane half-chair conformations. In these cases, however, the rings are far less puckered with twist angles of 26, 26° (catenane AB) and 28, 29° (catenane CD).

While the two [2]catenanes are of identical composition, it is through small conformational changes, and the resultant effect on intermolecular forces, that the inequivalence arises. In the first catenane (AB, Figure 4a) there are two close inter-ring Au ··· Au aurophilic attractions (3.216(2) and 3.357(2) Å), and four aryl – aryl interactions (two aryl – phenyl *ef*, two phenyl – phenyl *off*). In the second catenane (CD, Figure 4b), however, there is only one aurophilic interaction (Au(2C)–Au(2D) 3.231 Å), but there are five aryl – aryl attractions (four aryl – phenyl *ef*, one phenyl – phenyl *off*)—the other Au ··· Au distance (Au(1C)-Au(1D) 3.686(2) Å) is beyond the normal range of 2.75 – 3.40 Å for such bonds.[11]

Table 4. Selected bond lengths [Å] and bond angles [°] for [2]catenane complex **5a**.

| | | | |
|---|---|---|---|
| Au(1A)–P(1A) | 2.282(6) | Au(1B)–P(1B) | 2.269(8) |
| Au(2A)–P(2A) | 2.298(7) | Au(2B)–P(2B) | 2.272(8) |
| Au(1A)–C(11A) | 2.01(3) | Au(1B)–C(11B) | 2.02(4) |
| Au(2A)–C(33A) | 2.01(3) | Au(2B)–C(33B) | 1.97(3) |
| C(11A)–C(12A) | 1.17(4) | C(11B)–C(12B) | 1.21(4) |
| C(33A)–C(32A) | 1.18(3) | C(33B)–C(32B) | 1.22(3) |
| P(1A)-Au(1A)-C(11A) | 170.0(9) | P(1B)-Au(1B)-C(11B) | 166.3(10) |
| P(2A)-Au(2A)-C(33A) | 170.5(8) | P(2B)-Au(2B)-C(33B) | 171.6(8) |
| Au(1A)-C(11A)-C(12A) | 173(7) | Au(1B)-C(11B)-C(12B) | 173(3) |
| Au(2A)-C(33A)-C(32A) | 173(7) | Au(2B)-C(33B)-C(32B) | 167(3) |
| Au(1C)-P(1C) | 2.290(7) | Au(1D)-P(1D) | 2.271(7) |
| Au(2C)-P(2C) | 2.269(7) | Au(2D)-P(2D) | 2.285(7) |
| Au(1C)-C(11C) | 2.01(2) | Au(1D)-C(11D) | 1.96(3) |
| Au(2C)-C(33C) | 2.00(3) | Au(2D)-C(33D) | 2.00(3) |
| C(11C)-C(12C) | 1.19(3) | C(11D)-C(12D) | 1.26(3) |
| C(33C)-C(32C) | 1.17(3) | C(33D)-C(32D) | 1.23(3) |
| P(1C)-Au(1C)-C(11C) | 170.9(7) | P(1D)-Au(1D)-C(11D) | 174.9(8) |
| P(2C)-Au(2C)-C(33C) | 172.3(8) | P(2D)-Au(2D)-C(33D) | 172.2(9) |
| Au(1C)-C(11C)-C(12C) | 178(3) | Au(1D)-C(11D)-C(12D) | 178(2) |
| Au(2C)-C(33C)-C(32C) | 173(3) | Au(2D)-C(33D)-C(32D) | 169(2) |

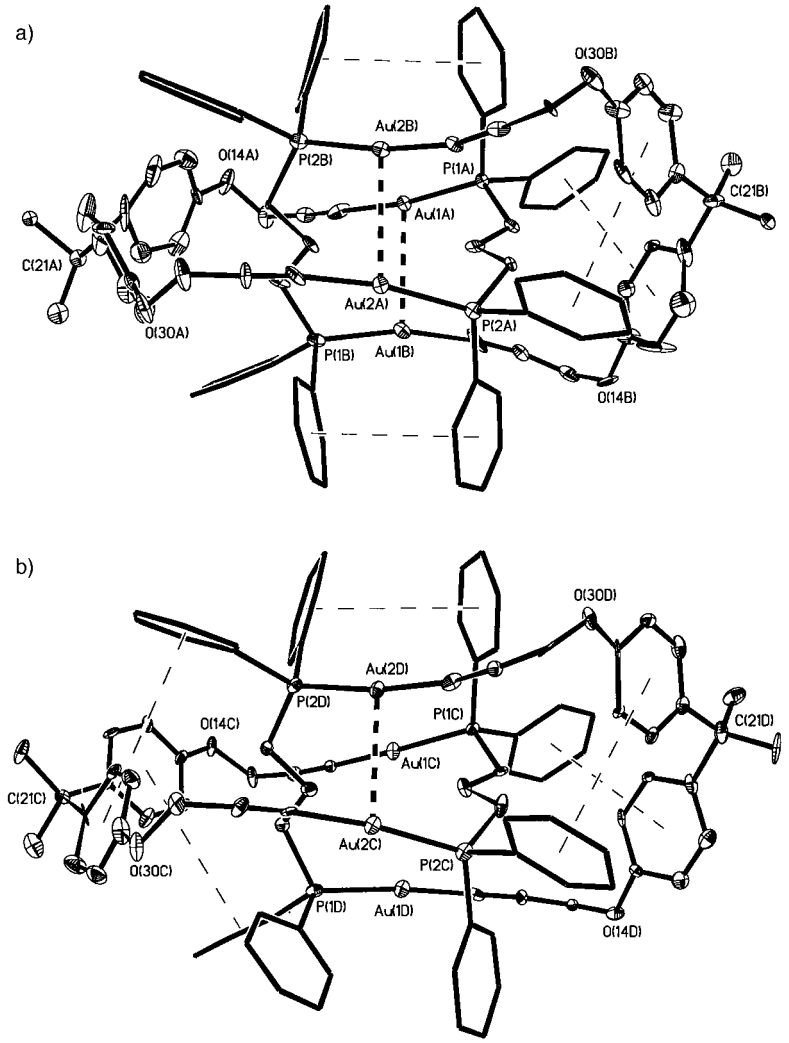


Figure 4. a, b) Views of the two independent [2]catenane structures of 5a. Dotted lines indicate secondary Au ··· Au or aryl ··· aryl bonds.

Clearly, in either case the sum of these secondary bonding forces overcomes the unfavorable entropy associated with formation of the [2]catenane and provides the driving force for the "2+2" self-assembly process. The presence of short gold ··· gold contacts in **5a** is mandatory within the small tightly intertwined catenane and, since the Au ··· Au interaction is attractive, it is naturally present. Since the two conformers present in the solid state must have very similar energies, there is a balance between maximizing the Au ··· Au or aryl ··· aryl attractive forces. In the less sterically demanding catenane **5b**, aurophilic interactions are not present in the solid state structure (longer Au ··· Au inter-ring distances) and there are a greater number of aryl – aryl attractions present.[15] It is relevant to note that aryl – aryl interactions have previously been identified as playing an important role in the self-assembly of organic catenane complexes.[2, 17]

**Luminescence properties of the macrocyclic gold(I) complexes**: The photophysical properties of the gold – acetylide rings (**4a – e**) and catenanes (**5a – c**) were studied and are summarized in

Table 5. All the synthesized complexes exhibit luminescence at room temperature, as solids in KBr and as solutions in $CH_2Cl_2$. Upon excitation at 325 nm, all the macrocyclic complexes display a single broad emission band in the range 375–378 nm in solution. In the solid state, however, excitation

Table 5. Photophysical data and Au···Au distances for cyclic gold complexes.

| Compound | Medium | $\lambda_{ex}$ [nm] | $\lambda_{em}$ [nm] | $d$(Au···Au) [Å] |
|---|---|---|---|---|
| **4a** | KBr | 345 | 446 | 2.9688(8) |
| | $CH_2Cl_2$ | 325 | 378 | |
| **4c** | KBr | 345 | 467 | 2.9887(13) |
| | $CH_2Cl_2$ | 325 | 376 | |
| **4d** | KBr | 345 | 467 | 2.9961(11) |
| | $CH_2Cl_2$ | 325 | 376 | |
| **4e** | KBr | 345 | 467 | |
| | $CH_2Cl_2$ | 325 | 376 | |
| **5a** | KBr | 345 | 427 | 3.216(2),3.357(2) |
| | $CH_2Cl_2$ | 325 | 375 | 3.231(2),3.686(2) |
| **5b** | KBr | 345 | 427 | 4.993(1),5.219(1) |
| | $CH_2Cl_2$ | 325 | 378 | |
| **5c** | KBr | 345 | 415 | |
| | $CH_2Cl_2$ | 325 | 375 | |

of the digold(I) diacetylide complexes at 345 nm results in a single broad emission band in the range 415–467 nm, a significant red shift. It has been previously reported that formation of Au···Au and aryl–aryl interactions in the solid state can lead to the observation of a red shift in the emission band compared to that in the solution phase.[8c, 18] For the present complexes, the red shift from solution to solid lies in the range 68–91 nm for the simple rings (**4a**–**e**), and 40–52 nm for the [2]catenanes (**5a**–**c**), suggesting stronger secondary interactions in the simple ring compounds in the solid state than in the solution phase. These observations can be correlated with structural data; the simple ring crystal structures are dominated by short intermolecular aurophilic interactions and supported by aryl–aryl attractions, while the [2]catenane structures are dominated by the aryl–aryl interactions and supported, in some cases, by weaker intramolecular aurophilic attractions (typical aryl–aryl attractions have energies of about 6 kJ mol$^{-1}$, compared to 7–11 kJ mol$^{-1}$ for Au···Au interactions).

**The equilibrium present for the bis(diphenylphosphanyl)propane (dppp) complex**: The initial product of reaction of **3** with dppp was a complex mixture, but recrystallization gave the pure [2]catenane **5a**. Complex **5a** could be characterized both in the solid state and in solution but, over a period of several days in solution, it slowly reacted to give back the original mixture of compounds. The mixture of products is thought to be that shown in Scheme 3, and the evidence will be discussed below.

Figure 5 shows the $^{31}$P NMR spectra of solutions of complex **5a** that were allowed to reach equilibrium over a period of one week at room temperature. The singlet resonance at $\delta = 31.9$ is due to the [2]catenane. As the isomerization occurred, three new resonances grew at $\delta = 35.9$, assigned to the simple ring complex **4b**, at $\delta = 34.7$, assigned to the 'double-ring' complex **6**, and a broad resonance at $\delta = 34.9$, assigned to a higher mass complex **7** (Scheme 3), whose structure is not known. Figure 5 contains spectra of solutions at four different concentrations. The relative concentrations of **5a** and **6** are independent of concentration; however, the relative concentration of the simple ring complex **4b** increases at lower concentrations (most abundant complex in the spectrum of Figure 5d) and that of **7** increases at higher concentration (most abundant complex in the spectrum of Figure 5a). Inspection of Figure 5 also shows that the linewidth of the resonance for complex **5a** is independent of concentration, whereas the other resonances are broader at higher concentrations. The peak broadening arises from rapid chemical exchange between these compounds.

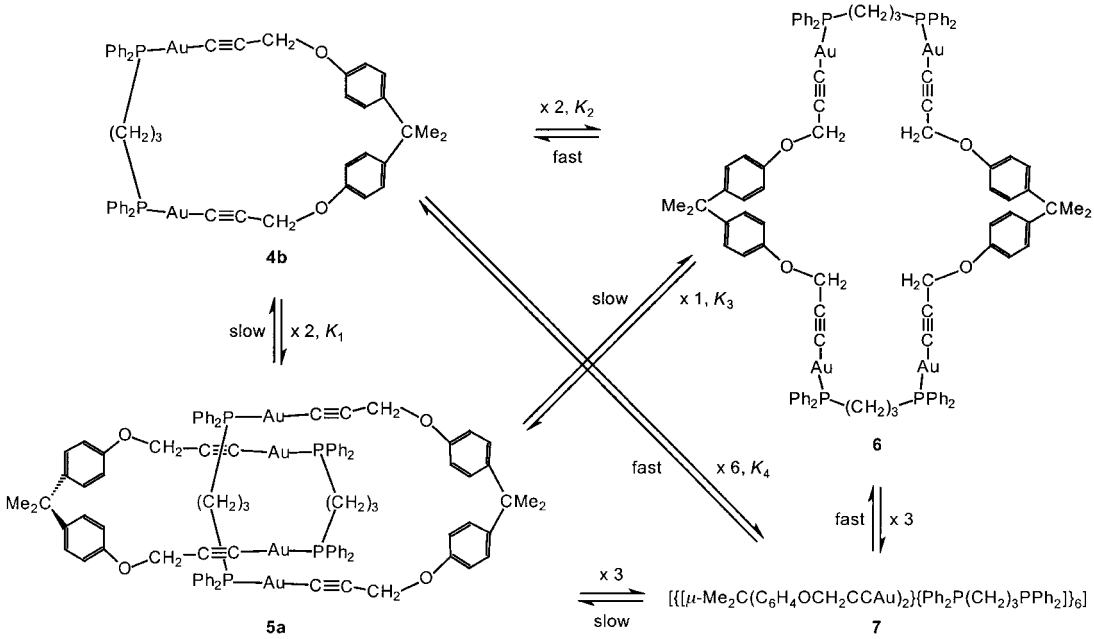


Scheme 3. The equilibria between rings **4b** and **6**, catenane **5a**, and unknown structure **7**.



0947-6539/02/0803-0728 $ 17.50+.50/0 *Chem. Eur. J.* **2002**, *8*, No. 3

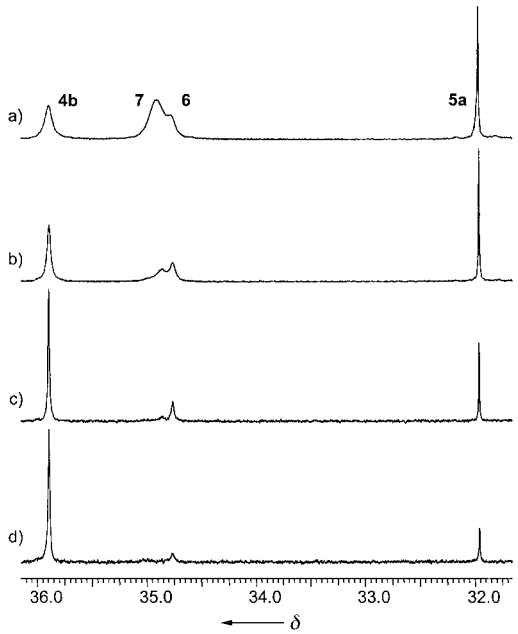


Figure 5. $^{31}$P NMR spectra at 20 °C of [2]catenane **5a** in equilibrium with its "isomers" **4b**, **6**, and **7** as a function of concentration. Total initial concentration of **5a** (before equilibration) was a) $48.5 \times 10^{-3}$ M, b) $24.2 \times 10^{-3}$ M, c) $12.1 \times 10^{-3}$ M, d) $2.3 \times 10^{-3}$ M.

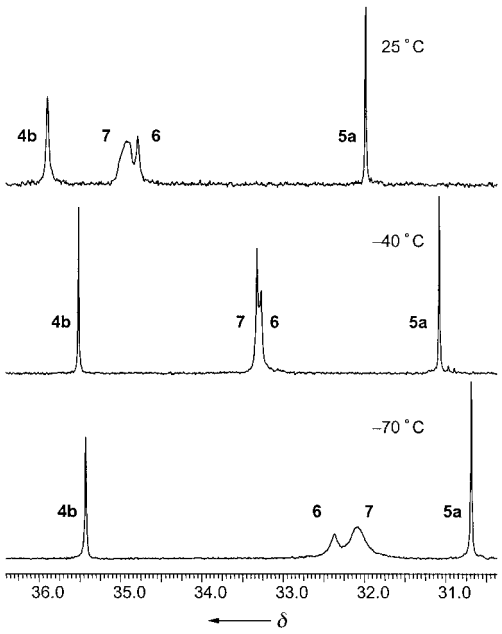


Figure 6. $^{31}$P NMR spectra of [2]catenane **5a** and its "isomers" **4b**, **6**, and **7** as a function of temperature. Total initial concentration of **5a** (before equilibration) was $35 \times 10^{-3}$ M.

By integration of the $^{31}$P resonances at different initial concentrations of **5a** ranging from $2.3 - 48.5 \times 10^{-3}$ M, it was possible both to determine the relative molar masses of the different components of the reaction mixture and to estimate the relevant equilibrium constants. At 20 °C, the corresponding values for formation of the [2]catenane **5a** or double-ring complex **6** from the simple ring **4b** are $K_1 = [\mathbf{5a}]/[\mathbf{4b}]^2 = 25.5(1.0)$ M$^{-1}$; $K_2 = [\mathbf{6}]/[\mathbf{4b}]^2 = 20(2)$ M$^{-1}$. It follows that $K_3 = [\mathbf{5a}]/[\mathbf{6}] = 1.3(0.1)$, showing that the double-ring and [2]catenane isomers **6** and **5a** have similar energies. The equilibrium to give **7** is less well defined, partly because the concentration of **7** at low overall concentration is too low to measure accurately and partly because of overlap with the resonance for complex **6** at higher concentrations. The best fit was that **7** is a hexamer of the simple ring with $K_4 = [\mathbf{7}]/[\mathbf{4b}]^6 = 1.8(0.2) \times 10^9$ M$^{-5}$. Since **7** is the most abundant complex at high concentrations, attempts were made to grow crystals under these conditions for positive structural characterization, but crystals of **5a** were obtained in each case.

Variable-temperature $^{31}$P NMR spectra for one sample are shown in Figure 6. The samples were equilibrated for several hours before recording the spectra, but the [2]catenane **5a** isomerizes only slowly so it is not at equilibrium with the other complexes under these conditions. The following observations can be made. First, it is clear from Figure 6 that the chemical shifts, especially for **6** and **7**, are temperature dependent. Going from 25 °C to −40 °C, the resonances for **4b**, **6**, and **7** become sharper as the intermolecular chemical exchange between them is slowed. However, between −40 C and −70 °C, the resonances for **6** and **7** broaden again. It is likely that each has a ground state conformation with different $^{31}$P environments, and that they become equivalent by intramolecular exchange. However, no splitting of the resonances to give separate peaks was observed at temperatures down to −90 °C. What is less clear from inspection of Figure 6, but which is clearly seen from the integration data, is that as the temperature is lowered the concentration of **7** increases, while the concentration of **4b** decreases. This is expected, since entropy effects will favor **4b** (monomer) > **5a**, **6** (dimers) > **7** (hexamer).

The easy intermolecular chemical exchange between **4b**, **6** and **7** was confirmed by recording the $^{31}$P NMR EXSY spectra and selected examples are shown in Figure 7. Since no chemical exchange was detected for the [2]catenane **5a**, that region of the spectrum is not shown in Figure 7. The spectra shown in Figure 7a–c were obtained on the same sample under different conditions. The spectra shown in Figure 7a and b were obtained at 20 °C, with mixing times of 200 and 50 ms, respectively. In the spectrum shown in Figure 7a chemical exchange is indicated between all pairs **4b**, **7**; **4b**, **6**; **6**, **7** but in in Figure 7b the chemical exchange cross peak between **6**, **7** is absent and those for **4b**, **7**; **4b**, **6** are much weaker. Overall, the ease of exchange follows the series **4b**, **6** > **4b**, **7** > **6**, **7** ≫ > **4b**, **5a**; **5a**, **6**; **5a**, **7** under these conditions. The spectra shown in Figure 7a and c were both recorded using a mixing time of 200 ms but that in Figure 7c was obtained at −40 °C. Under these conditions, the chemical shifts for **6** and **7** are close together (compare Figure 6), but no chemical exchange is detected at the low temperature. Finally, the spectra shown in Figure 7a and d were each recorded using mixing times of 200 ms, but the overall concentration was lower than for the spectrum shown in Figure 7d. Under these conditions, exchange between **4b** and **6** is still clear but the exchange between **4b** and **7** is barely detected. This difference arises since there is a greater concentration dependence for exchange with the hexamer **7**, and the effect is accentuated because the concentration of **7** is lower at the lower concentration.

  0947-6539/02/0803-0729 $ 17.50+.50/0 

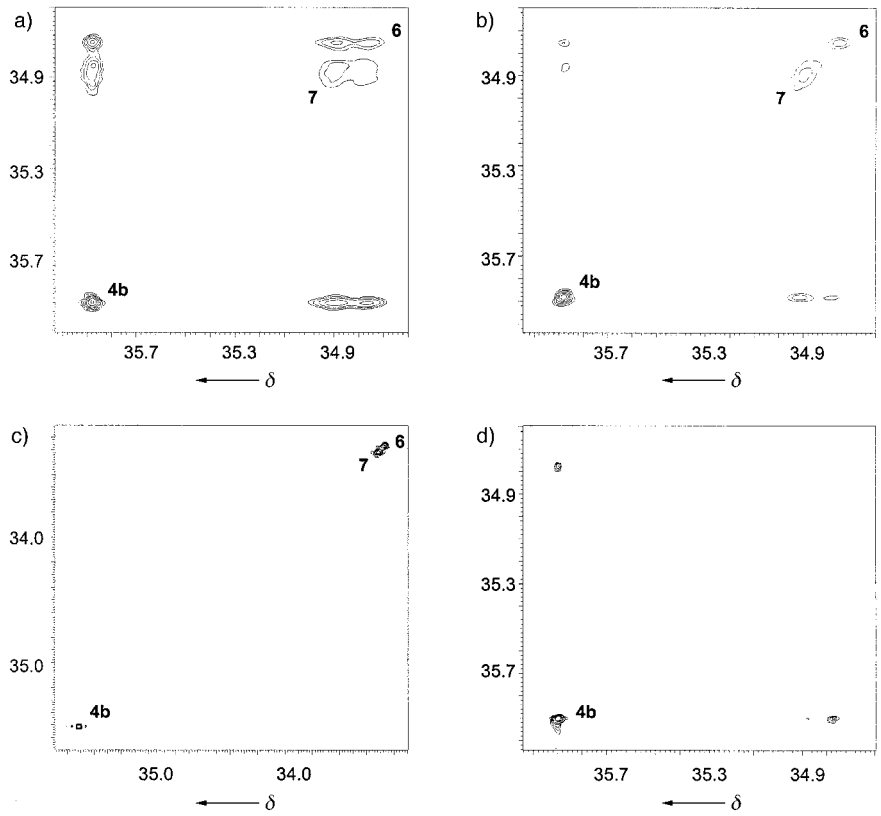


Figure 7. $^{31}P$ 2D EXSY NMR spectra **4b**, **6**, and **7** as a function of total concentration $c$, temperature $T$, and mixing time $t$. Values of $c$, $T$, $t$ are: a) $35 \times 10^{-3}$ M, 20 °C, 200 ms; b) $35 \times 10^{-3}$ M, 20 °C, 50 ms; c) $35 \times 10^{-3}$ M, −40 °C, 200 ms; d) $7 \times 10^{-3}$ M, 20 °C, 200 ms. See the text for details.

Many of the above conclusions were confirmed from the corresponding $^{1}H$ and $^{13}C$ NMR spectra, including correlated $^{1}H$-$^{1}H$, $^{1}H$-$^{13}C$, $^{1}H$-$^{31}P$, and $^{13}C$-$^{31}P$ NMR spectra. $^{1}H$-$^{1}H$ NOESY spectra confirmed the chemical exchange (negative cross peaks observed) with a similar time constant $\tau \approx 100$ ms, as found in the $^{31}P$ EXSY spectra for exchange between **4b** and **6**. The crowded structure of the [2]catenane leads to some unusual chemical shifts in the $^{1}H$ NMR spectra. For example the *ortho*-hydrogen atoms of the PhP groups occur at $\delta = 7.15$ for **5a** but at 7.56 for **6** and 7.48 for **4b**. The AA′XX′ signals for the $C_6H_4O$ groups are at $\delta = 6.77, 6.13$ for **5a**; 7.12, 6.92 for **4b**; 6.96, 6.78 for **6** and 6.99, 6.79 for **7**. The $^{1}H$ resonances for **7** were broad and complete assignment was not possible, and no useful additional structural information was obtained. It could be a giant ring or a complex catenane or it could have a more complex topological form such as a knot. The largest structure previously identified from similar reactions was the doubly braided catenane, which was considered a tetramer $[Au_2(\text{diacetylide})(\text{diphosphane})]_4$, but its spectral properties are distinct from those of **7**.[13, 15]

The equilibria described are complex but they give a rare opportunity to observe the interchange between ring and [2]catenane structures.[19] An unexpected feature is the great differences in rates for the equilibria involving **5a** (several days at room temperature) compared with those involving only **4b**, **6** and **7** (fractions of a second at room temperature). The slow reactions of **5a** are attributed to the very compact structure in which the gold atoms are sterically protected in the [2]catenane core. The mechanism(s) of interconversion are not easy to determine. However, the equilibria involving **5a** are found to be greatly accelerated in the presence of free diphosphane ligand and so it is likely that the reactions are associative under these conditions. It is likely that the diphosphane attacks at gold(I) with ring opening, leading to the formation of linear molecules with monodentate diphosphane or diacetylide ligands, and that these ring-opened intermediates undergo threading or dethreading to make or break the [2]catenane structure, or take part in ring expansion or contraction.

**Mixed-phosphane reactions**: In an attempt to synthesize a mixed-ligand [2]catenane, the oligomer **3**, was allowed to react with all seven pairwise combinations of the diphosphanes $Ph_2P(CH_2)_xPPh_2$ $(x = 2-5)$. In each case, 0.5 equivalents of both phosphanes were used, and the reaction products were isolated and characterized by $^{1}H$, $^{13}C$, and $^{31}P$ NMR techniques.

Throughout all seven reactions, not one single mixed-ligand product was obtained; each reaction yielded the two homorecognition products (rings and [2]catenanes, **4a** and **5a**–**c**, with the complex equilibrium in the case of dppp), as would be expected for the individual phosphane reactions. Similarly, mixing of two pure [2]catenanes, such as **5b** and **5c**, failed to give any detectable amount of the expected unsymmetrical [2]catenane. These surprising results demonstrate that there is a high degree of selectivity present in this gold–phosphane self-assembly process, which is clearly an excellent example of molecular recognition. While a mixed catenane involving the short dppe ligand is likely disfavored on steric grounds, this should not be the case with combinations of the longer diphosphanes, which can form homo[2]catenanes in their own right. A possible explanation for these observations is that the potential mixed-ligand catenanes might not have the conformational ability to maximize intramolecular attractions.

**Chiral acetylide reactions**: It was hoped that by starting with a chiral bisphenol derivative with a similar structure to the bisphenol **1**, analogous methodology would allow the synthesis and isolation of chiral [2]catenanes.[20] These new products could exhibit both simple chirality and topological chirality and, by using a racemic mixture of starting material, any stereoselectivity in catenane formation would become apparent.



0947-6539/02/0803-0730 $ 17.50+.50/0 *Chem. Eur. J.* **2002**, *8*, No. 3

A racemic mixture of the chiral bisphenol **8** was used to synthesize the bis(acetylide) derivative **9**, which was subsequently used to form the chiral digold(I) diacetylide oligomer **10** (Scheme 4). The oligomer **10**, was then treated with the diphosphane ligands, $Ph_2P(CH_2)_xPPh_2$ ($x = 2-5$) to yield four new macrocyclic products, **11a–d** (Scheme 4). All the new products (air-stable white solids that slowly decompose in solution) were characterized by IR and NMR spectroscopy, and by elemental analysis—no crystals suitable for X-ray crystallographic analysis could be obtained. The data for all four complexes were fully assigned, and are listed in the Experimental Section.

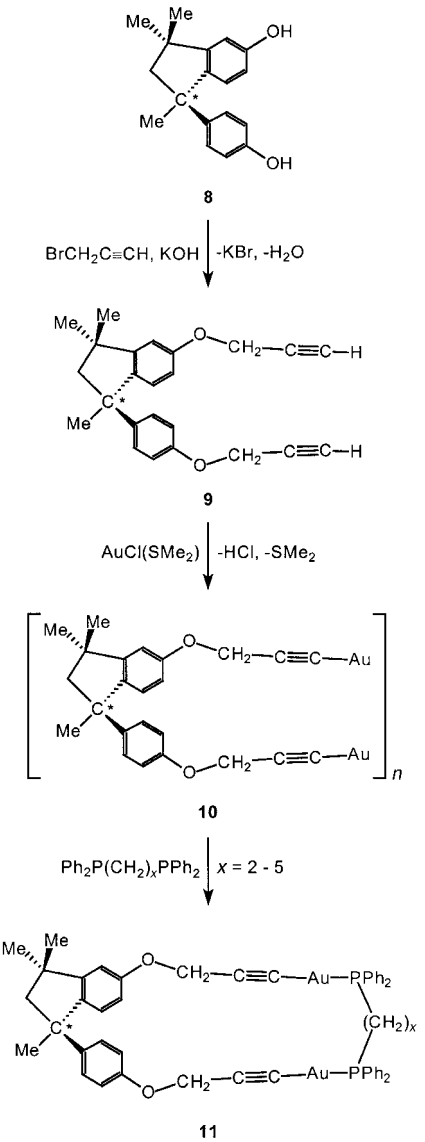


Scheme 4. Synthesis of **11** from **8**.

It is clear from the $^{31}P$ NMR data, that all four products are simple ring structures, with only two singlet resonances being observed in each spectrum. If a [2]catenane product was formed, four or eight signals are expected in the $^{31}P$ NMR spectra, depending upon the stereoselectivity of the catenane formation. Similarly in the $^{1}H$ NMR spectra, only two AB quartets are observed for the inequivalent $OCH_2$ protons. Each product macrocycle will exist as a racemic mixture of a chiral simple ring structure. Clearly the structural changes in the bisphenol backbone, compared to **1**, have affected the ability of the digold(I) diacetylide **9** to undergo catenane formation. It is probable that the increased steric effects will hinder the ability to form the aryl–aryl interactions that are necessary to overcome the unfavorable entropy of catenane formation.

## Conclusion

The reactions of digold(I) diacetylides $X(C_6H_4OCH_2CCAu)_2$ with diphosphane ligands can give either simple ring complexes or [2]catenanes, depending on the nature of the hinge group X or the spacer group in the diphosphane ligand. The reactions are significant since they occur very easily and in high yield, and since the products contain the first family of organometallic [2]catenanes. The dependence of selectivity of self-assembly on the hinge group X has been reported previously,[15] while the present work is focussed on how selectivity depends on the spacer group of the diphosphane ligand, using the single hinge group $CMe_2$. There is a very sharp switch in the selectivity of self-assembly for the diphosphanes $Ph_2P(CH_2)_xPPh_2$ as a function of $x$, and only when $x = 3$ is there an equilibrium present. The shorter bite diphosphane $Ph_2P(CH_2)_2PPh_2$ gives only the simple ring form by 1+1 self-assembly, while the longer bite diphosphanes $Ph_2P(CH_2)_xPPh_2$, with $x = 3$ or 4, give only the [2]catenane by 2+2 self-assembly. This study, together with parallel work,[15] provides a sound basis for the design of other organometallic [2]catenanes.

## Experimental Section

NMR spectra were recorded using Varian Mercury 400 and Inova 600 MHz spectrometers. $^{1}H$ and $^{13}C$ NMR chemical shifts are reported relative to tetramethylsilane, while $^{31}P$ chemical shifts are reported relative to 85% $H_3PO_4$ as an external standard. IR spectra were recorded using a Perkin-Elmer 2000 FTIR as Nujol mulls on KBr plates or as $CH_2Cl_2$ solutions in 0.1 mm NaCl cell. Emission spectra were recorded at room temperature using a Fluorolog-3 spectrofluorimeter. For recording the emission and excitation spectra, solutions were placed in quartz cuvettes, while solid samples were ground finely with added KBr. All gold complexes were protected from light by using darkened reaction flasks.

MALDI-TOF data were acquired using a Micromass TofSpec 2E mass spectrometer in positive-ion mode. The samples were dissolved in $CHCl_3$ (1 mg mL$^{-1}$) and mixed 1:1 with the matrix solution (dihydroxybenzoic acid 10 mg mL$^{-1}$ in $CHCl_3$/MeOH 50:50) prior to application on the target. The samples were analyzed in reflectron mode and MS spectra were externally calibrated with a peptide mix (bradykinin, angiotensin I, renin substrate and ACTH18–39).

Compounds **2**, **3**,and **5b**, were prepared by experimental procedures as previously reported.[15] The complex $[AuCl(SMe_2)]$ was prepared by the literature method.[21]

**Caution**: Some gold acetylides are potentially explosive; they should be prepared in small quantities and not subjected to shock!

**$[Au_2\{(CCCH_2OC_6H_4)_2CMe_2\}(Ph_2P(CH_2)_2PPh_2)]$ (4a)**: A mixture of **3** (0.125 g, 0.180 mmol) and $Ph_2P(CH_2)_2PPh_2$ (0.079 g, 0.198 mmol) in $CH_2Cl_2$ (50 mL) was stirred for 3 h at room temperature. Activated charcoal was added to the solution, which was stirred for a further 0.5 h then filtered. The

filtrate was concentrated (ca. 1–2 mL) and addition of pentane (100 mL) precipitated a white solid. The powder was collected by filtration, washed with diethyl ether and pentane, and dried. Yield 0.137 g, 70%. IR ($CH_2Cl_2$): $\tilde{\nu}$ = 2130 (w) $cm^{-1}$ (C≡C); $^1H$ NMR (400 MHz, $CD_2Cl_2$, 25 °C): $\delta$ = 7.50–7.44 (m, 20H; Ph), 7.23 (m, 4H; $C_6H_4$), 7.00 (m, 4H; $C_6H_4$), 4.75 (s, 4H; $OCH_2$), 2.51 (m, 4H; $CH_2$), 1.65 (s, 6H; Me); $^{31}P$ NMR (160 MHz, $CD_2Cl_2$, 25 °C): $\delta$ = 40.54; $^{13}C$ NMR (100 MHz, $CD_2Cl_2$, 25 °C): $\delta$ = 156.0, 143.5 (both $C_6H_4$), 133.6, 129.6, 132.3 (all Ph), 129.3 (C≡C), 127.6, 114.8 (both $C_6H_4$), 97.8 (C≡C), 56.5 ($OCH_2$), 41.5 ($CMe_2$), 30.8 (Me), 24.1 ($CH_2$); elemental analysis calcd (%) for $C_{47}H_{42}Au_2P_2O_2$ (1094.7): C 51.57, H 3.87; found: C 52.04, H 3.95. X-ray quality crystals were grown from slow diffusion of $Et_2O$ into a solution of complex **4a** in $CH_2Cl_2$.

**[$Au_2${($CCCH_2OC_6H_4)_2CMe_2$}($Ph_2P(CH_2)_2PPh_2)_2$]**: An insoluble white solid [$Au_2${($CCCH_2OC_6H_4)_2CMe_2$}($Ph_2P(CH_2)_2PPh_2)_2$] was similarly prepared from **3** (0.100 g, 0.144 mmol) and excess $Ph_2P(CH_2)_2PPh_2$ (0.250 g, 0.628 mmol). Yield 0.157 g; elemental analysis calcd (%) for $C_{73}H_{66}Au_2P_4O_2$ (1493.2): C 58.72, H 4.46; found: C 58.76, H 4.44.

**[$Au_2${($CCCH_2OC_6H_4)_2CMe_2$}($Ph_2PCCPPh_2$)] (4c)**: This was prepared similarly from **3** (0.100 g, 0.144 mmol) and $Ph_2PC{\equiv}CPPh_2$ (0.051 g, 0.130 mmol). The product was isolated as a white solid. Yield 0.107 g, 76%. IR ($CH_2Cl_2$): $\tilde{\nu}$ = 2134 (w) $cm^{-1}$ (C≡C); $^1H$ NMR (400 MHz, $CD_2Cl_2$, 25 °C): $\delta$ = 7.76–7.50 (m, 20H; Ph), 7.19 (m, 4H; $C_6H_4$), 7.00 (m, 4H; $C_6H_4$), 4.77 (s, 4H; $OCH_2$), 1.63 (s, 6H; $CH_3$); $^{31}P$ NMR (160 MHz, $CD_2Cl_2$, 25 °C): $\delta$ = 18.93; $^{13}C$ NMR (100 MHz, $CD_2Cl_2$, 25 °C): $\delta$ = 156.2, 143.5 (both $C_6H_4$), 133.6, 132.8, 129.9 (all Ph), 128.0 (d, $^1J_{P,C}$ = 63 Hz; Ph), 127.8, 114.6 (both $C_6H_4$), 101.4 (d, $^1J_{P,C}$ = 85 Hz; PC≡CP), 98.1 (C≡C), 56.8 ($OCH_2$), 41.8 ($CMe_2$), 31.1 (Me); elemental analysis calcd (%) for $C_{47}H_{38}Au_2P_2O_2$ (1090.7): C 51.76, H 3.51; found: C 51.44, H 3.44. X-ray quality crystals were grown from slow diffusion of $Et_2O$ into a solution of complex **4c** in $CH_2Cl_2$.

**[$Au_2${($CCCH_2OC_6H_4)_2CMe_2$}(*trans*-$Ph_2PCH{=}CHPPh_2$)] (4d)**: This was prepared similarly from **3** (0.100 g, 0.144 mmol) and *trans*-[$Ph_2PCH{\equiv}CHPPh_2$] (0.051 g, 0.129 mmol). The product was isolated as a white solid. Yield 0.114 g, 81%. IR ($CH_2Cl_2$): $\tilde{\nu}$ = 2129 (w) $cm^{-1}$ (C≡C); $^1H$ NMR (400 MHz, $CD_2Cl_2$, 25 °C): $\delta$ = 7.56–7.46 (m, 20H; Ph), 7.20 (m, 4H; $C_6H_4$), 6.99 (m, 4H; $C_6H_4$), 6.87 (m, 2H; CH=CH), 4.74 (s, 4H, $OCH_2$), 1.63 (s, 6H, $CH_3$); $^{31}P$ NMR (160 MHz, $CD_2Cl_2$, 25 °C): $\delta$ = 39.65; $^{13}C$ NMR (100 MHz, $CD_2Cl_2$, 25 °C): $\delta$ = 156.1, 143.5 (both $C_6H_4$), 141.1, 140.9 (both CH), 134.3, 132.6, 129.8 (all Ph), 128.3 (d, $^2J_{P,C}$ = 28 Hz; C≡C), 127.7, 114.7 (both $C_6H_4$), 97.9 (C≡C), 56.6 ($OCH_2$), 41.6 ($CMe_2$), 31.0 (Me); elemental analysis calcd (%) for $C_{47}H_{40}Au_2P_2O_2$ (1092.7): C 51.66, H 3.69; found: C 51.47, H 3.63. X-ray quality crystals were grown from slow diffusion of $Et_2O$ into a solution of complex **4d** in $CH_2Cl_2$.

**[$Au_2${($CCCH_2OC_6H_4)_2CMe_2$}{($Ph_2PC_5H_4)_2Fe$}] (4e)**: This was prepared similarly from **3** (0.120 g, 0.172 mmol) and [$Fe(C_5H_4PPh_2)_2$] (0.080 g, 0.144 mmol). The product was isolated as a yellow solid. Yield 0.135 g, 75%. IR ($CH_2Cl_2$): $\tilde{\nu}$ = 2134 (w) $cm^{-1}$ (C≡C); $^1H$ NMR (400 MHz, $CD_2Cl_2$, 25 °C): $\delta$ = 7.54–7.41 (m, 20H; Ph), 7.22 (m, 4H; $C_6H_4$), 6.99 (m, 4H; $C_6H_4$), 4.81 (s, 4H; $OCH_2$), 4.40 (s, 8H; $C_5H_4$), 1.65 (s, 6H; $CH_3$); $^{31}P$ NMR (160 MHz, $CD_2Cl_2$, 25 °C): $\delta$ = 37.06; $^{13}C$ NMR (100 MHz, $CD_2Cl_2$, 25 ?C): $\delta$ = 156.1, 143.4 (both $C_6H_4$), 133.9, 131.8 (both Ph), 131.3 (C≡C), 129.3 (Ph), 127.7, 114.8 (both $C_6H_4$), 97.8 (C≡C), 75.2 ($C_5H_5$), 56.6 ($OCH_2$), 41.6 ($CMe_2$), 30.7 (Me); elemental analysis calcd (%) for $C_{55}H_{46}Au_2P_2O_2Fe_1$ (1250.7): C 52.82, H 3.71; found: C 52.20, H 3.64.

**[{$Au_2${($CCCH_2OC_6H_4)_2CMe_2$}($Ph_2P(CH_2)_3PPh_2$)}$_2$] (5a)**: This was prepared similarly from **3** (0.140 g, 0.201 mmol) and $Ph_2P(CH_2)_3PPh_2$ (0.091 g, 0.221 mmol). The product was isolated as a white solid. Yield 0.180 g, 81%. The initial product is a mixture of isomers but recrystallization gave the pure [2]catenane, whose data are given. IR ($CH_2Cl_2$): $\tilde{\nu}$ = 2132 (w) $cm^{-1}$ (C≡C); $^1H$ NMR (400 MHz, $CD_2Cl_2$, 25 °C): $\delta$ = 7.45–7.17 (m, 40H; Ph), 6.77 (m, 8H; $C_6H_4$), 6.13 (m, 8H; $C_6H_4$), 4.55 (s, 8H; $OCH_2$), 2.32 (m, 4H; $CH_2$), 1.82 (m, 8H, $CH_2$), 1.42 (s, 12H; Me); $^{31}P$ NMR (160 MHz, $CD_2Cl_2$, 25 °C): $\delta$ = 31.67; $^{13}C$ NMR (100 MHz, $CD_2Cl_2$, 25 °C): $\delta$ = 155.5, 143.0 (both $C_6H_4$), 133.7, 131.0, 129.5 (all Ph), 127.1, 115.1 (both $C_6H_4$), 56.9 ($OCH_2$), 40.8 ($CMe_2$), 30.5 (Me), 28.3, 22.8 (both $CH_2$); elemental analysis calcd (%) for $C_{96}H_{88}Au_4P_4O_4$ (2217.5): C 52.00, H 4.00; found: C 52.15, H 4.10. The $^{31}P$ NMR spectrum of the initial product contained additional resonances: ($^{31}P$ NMR): $\delta$ = 35.61 (s, simple ring **4e**), 34.56 (br, unknown complex **6**), 34.47 (br, unknown complex **7**); the pure catenane in solution reverted to the equilibrium mixture over a period of 5–6 days.

**[$Au_2${($CCCH_2OC_6H_4)_2CMe_2$}($Ph_2P(CH_2)_5PPh_2$)] (5c)**: This was prepared similarly from **3** (0.127 g, 0.182 mmol) and $Ph_2P(CH_2)_5PPh_2$ (0.089 g, 0.202 mmol). The product was isolated as a white solid. Yield 0.145 g, 70%. IR ($CH_2Cl_2$): $\tilde{\nu}$ = 2130 (w) $cm^{-1}$ (C≡C); $^1H$ NMR (400 MHz, $CD_2Cl_2$, 25 °C): $\delta$ = 7.67–7.44 (m, 40H; Ph), 7.20 (m, 8H; $C_6H_4$), 6.99 (m, 8H; $C_6H_4$), 4.77 (s, 8H; $OCH_2$), 2.36 (m, 8H; $CH_2$), 1.65 (s, 12H; Me), 1.57 (m, 12H, $CH_2$); $^{31}P$ NMR (160 MHz, $CD_2Cl_2$, 25 °C): $\delta$ = 37.36; $^{13}C$ NMR (100 MHz, $CD_2Cl_2$, 25 °C): $\delta$ = 156.1, 143.5 (both $C_6H_4$), 133.6, 131.8 (both Ph), 131.0 (d, $^2J_{P,C}$ = 53 Hz; C≡C), 129.4 (Ph), 127.8, 114.7 (both $C_6H_4$), 97.7 (d, $^3J_{P,C}$ = 26 Hz; C≡C), 56.7 ($OCH_2$), 41.8 ($CMe_2$), 31.1 (Me), 28.1 (d, $^1J_{P,C}$ = 36 Hz; $CH_2$), 25.9, 25.0 (both $CH_2$); elemental analysis calcd (%) for $C_{100}H_{96}Au_4P_4O_4$ (2273.6): C 52.83, H 4.26; found: C 52.30, H 4.17.

**Chiral diacetylide ligand 9**: $BrCH_2C{\equiv}CH$ (2.66 g, 22.4 mmol) and finely ground KOH (1.35 g, 24.0 mmol) were added to a solution of **8** (2.0 g, 7.5 mmol) in acetone (50 mL). The mixture was heated at reflux for about 16 h. The solution was allowed too cool to room temperature then filtered to give a pale yellow filtrate. The solvent was removed under reduced pressure and the resultant pale yellow oil dried under vacuum (3 days). The product was washed with pentane and dried further. Yield: 2.12 g, 82%. IR (Nujol): $\tilde{\nu}$ = 2122 (m), 2050 (w) $cm^{-1}$ (C≡C); $^1H$ NMR (400 MHz, $CD_2Cl_2$, 25 °C): $\delta$ = 7.12 (m, 2H; $C_6H_4$), 7.11 (d, $^2J$ = 8.8 Hz, 1H; $C_6H_3$), 6.89 (dd, $^2J$ = 8.8 Hz, $^3J$ = 2.8 Hz, 1H; $C_6H_3$), 6.84 (m, 2H; $C_6H_4$), 6.68 (d, $^3J$ = 2.8 Hz, 1H; $C_6H_3$), 4.67 (d, $J$ = 2.4 Hz, 2H; $OCH_2$), 4.65 (d, $J$ = 2.4 Hz, 2H; $OCH_2$), 2.55 (m, 2H; CH), 2.37 (d, $J$ = 12.8 Hz, 1H; $CH_2$), 2.19 (d, $J$ = 12.8 Hz, 1H; $CH_2$), 1.64 (s, 3H; Me), 1.31 (s, 3H; Me), 1.02 (s, 3H; Me); $^{13}C$ NMR (100 MHz, $CD_2Cl_2$, 25 °C): $\delta$ = 157.2 ($C_6H_3$), 155.7 ($C_6H_4$), 150.8 ($C_6H_3$), 145.7 ($C_6H_3$), 144.2 ($C_6H_4$), 128.0 ($C_6H_4$), 123.6 ($C_6H_3$), 114.4 ($C_6H_4$), 114.4 ($C_6H_3$), 111.4 ($C_6H_3$), 79.2 (*C*≡CH), 79.1 (*C*≡CH), 75.4 (CH), 59.8 ($CH_2$), 56.3 ($OCH_2$), 56.0 ($OCH_2$), 50.4 (*C*Me), 42.5 (*C*$Me_2$), 30.9 (Me), 30.9 (Me), 30.5 (Me).

**Chiral digold(I) diacetylide 10**: [$AuCl(SMe_2)$] (0.345 g, 1.17 mmol) was dissolved in the mixed solvents THF (70 mL)/MeOH (25 mL). To the solution was then added a solution of **9** (0.202 g, 0.59 mmol) and $NaO_2CMe$ (0.240 g, 2.93 mmol) in THF (20 mL)/MeOH (20 mL). The resulting mixture was stirred for 16 h to produce a dark yellow precipitate. The solid was then collected by filtration, washed with THF, MeOH, $Et_2O$, and pentane, and dried. Yield: 0.264 g, 61%. The product is insoluble in common organic solvents. IR (Nujol): $\tilde{\nu}$ = 1995 (w, br) $cm^{-1}$ (C≡C); elemental analysis calcd (%) for $C_{24}H_{22}Au_2O_2$ (736.4): C 39.15, H 3.01; found: C 38.70, H 2.88.

**Simple ring 11a**: A mixture of **10** (0.120 g, 0.162 mmol) and $Ph_2P(CH_2)_2PPh_2$ (0.058 g, 0.147 mmol) in $CH_2Cl_2$ (50 mL) was stirred for 3 h at room temperature. Activated charcoal was added to the solution, which was stirred for a further 0.5 h then filtered. The filtrate was concentrated (ca. 1–2 mL) and addition of pentane (100 mL) precipitated a white solid. The powder was collected by filtration, washed with diethyl ether and pentane, and dried. Yield 0.134 g, 81%. IR (Nujol): $\tilde{\nu}$ = 2132 (w) $cm^{-1}$ (C≡C); $^1H$ NMR (600 MHz, $CD_2Cl_2$, 25 °C): $\delta$ = 7.60–7.36 (m, 20H; Ph), 7.16 (m, 2H; $C_6H_4$), 7.10 (m, 1H; $C_6H_3$), 7.07 (m, 2H; $C_6H_4$), 6.89 (m, 1H; $C_6H_3$), 6.82 (m, 1H; $C_6H_3$), 4.84, 4.79 (AB q, $J$ = 17.1 Hz, 2H; $OCH_2$), 4.76, 4.70 (AB q, $J$ = 17.1 Hz, 2H; $OCH_2$), 2.60 (m, 4H; [P]$CH_2$), 2.43 (d, $J$ = 12.6 Hz, 1H; $CH_2$), 2.15 (d, $J$ = 12.6 Hz, 1H; $CH_2$), 1.64 (s, 3H; Me), 1.30 (s, 3H; Me), 1.06 (s, 3H; Me); $^{31}P$ NMR (160 MHz, $CD_2Cl_2$, 25 °C): $\delta$ = 40.10 (s; P); $^{13}C$ NMR (150 MHz, $CD_2Cl_2$, 25 °C): $\delta$ = 157.9 ($C_6H_3$), 156.4 ($C_6H_4$), 151.3 ($C_6H_3$), 144.9 ($C_6H_3$), 143.2 ($C_6H_4$), 133.7 (m; Ph), 132.3 (s br; Ph), 129.6 (m; Ph), 127.7 ($C_6H_4$), 123.2 ($C_6H_3$), 115.4 ($C_6H_4$), 113.6 ($C_6H_3$), 112.4 ($C_6H_3$), 98.8 (m w, *C*≡CAu), 59.5 ($CH_2$), 57.4 ($OCH_2$), 56.9 ($OCH_2$), 50.4 (*C*Me), 42.4 (*C*$Me_2$), 31.2 (Me), 31.0 (Me), 30.4 (Me), 24.1(m, [P]$CH_2$); elemental analysis calcd (%) for $C_{50}H_{46}Au_2P_2O_2 \cdot 0.5CH_2Cl_2$ (1177.3): C 51.52, H 4.02; found: C 51.43, H 3.98.

**Simple ring 11b**: This was prepared similarly from **10** (0.120 g, 0.162 mmol) and $Ph_2P(CH_2)_3PPh_2$ (0.060 g, 0.147 mmol). The product was isolated as a white solid. Yield 0.119 g, 71%. IR (Nujol): $\tilde{\nu}$ = 2133 (w) $cm^{-1}$ (C≡C); $^1H$ NMR (400 MHz, $CD_2Cl_2$, 25 °C): $\delta$ = 7.78–7.37 (m, 20H; Ph), 7.21 (m, 2H; $C_6H_4$), 7.10 (m, 1H; $C_6H_3$), 7.00 (m, 2H; $C_6H_4$), 6.87 (s br, 1H; $C_6H_3$), 6.84 (m, 1H; $C_6H_3$), 4.79 (m, 1H; $OCH_2$), 4.72 (m, 1H; $OCH_2$), 4.64, 4.53 (AB q, $J$ = 16.4 Hz, 2H; $OCH_2$), 3.17 (m, 1H; $[P]_aCH_2$), 3.04 (m, 1H; $[P]_aCH_2$), 2.75 (m, 1H; $[P]_aCH_2$), 2.62 (m, 1H; $[P]_aCH_2$), 2.30 (d, $J$ = 12.8 Hz, 1H; $CH_2$), 2.19 (d, $J$ = 12.8 Hz, 1H; $CH_2$), 1.82 (m, 2H; $[P]_bCH_2$), 1.64 (s, 3H; Me), 1.33 (s, 3H; Me), 1.10 (s, 3H; Me); $^{31}P$ NMR (160 MHz, $CD_2Cl_2$, 25 °C): $\delta$ = 31.80 (s; P), 31.46 (s; P); $^{13}C$ NMR



0947-6539/02/0803-0732 $ 17.50+.50/0 *Chem. Eur. J.* **2002**, *8*, No. 3

(150 MHz, $CD_2Cl_2$, 25 °C): $\delta = 157.1$ ($C_6H_3$), 156.1 ($C_6H_4$), 150.8 ($C_6H_3$), 144.6 ($C_6H_3$), 143.4 ($C_6H_4$), 133.9 (m br; Ph), 131.7 (m; Ph), 129.5 (m; Ph), 127.8 ($C_6H_4$), 123.3 ($C_6H_3$), 116.0 ($C_6H_4$), 114.4 ($C_6H_3$), 110.8 ($C_6H_3$), 98.8 (m w; *C*≡CAu), 59.9 ($CH_2$), 57.5 ($OCH_2$), 56.7 ($OCH_2$), 50.6 (*C*Me), 42.5 (*C*$Me_2$), 31.5 (Me), 31.2 (Me), 31.0 (Me), 30.8(m, [P]$CH_2$), 28.7(m, [P]$CH_2$); elemental analysis calcd (%) for $C_{51}H_{48}Au_2P_2O_2 \cdot H_2O$ (1166.8): C 52.50, H 4.32; found: C 52.62, H 4.19.

**Simple ring 11c**: This was prepared similarly from **10** (0.125 g, 0.170 mmol) and $Ph_2P(CH_2)_4PPh_2$ (0.065 g, 0.152 mmol). The product was isolated as a white solid. Yield 0.145 g, 82 %. IR (Nujol): $\tilde{\nu} = 2133$ (w) $cm^{-1}$ (C≡C); $^1H$ NMR (600 MHz, $CD_2Cl_2$, 25 °C): $\delta = 7.66 - 7.37$ (m, 20H; Ph), 7.14 (m, 2H; $C_6H_4$), 7.11 (m, 1H; $C_6H_3$), 6.99 (m, 2H; $C_6H_4$), 6.93 (m, 1H; $C_6H_3$), 6.85 (m, 1H; $C_6H_3$), 4.83, 4.78 (AB q, $J = 15.6$ Hz, 2H; $OCH_2$), 4.72, 4.67 (AB q, $J = 15.6$ Hz, 2H; $OCH_2$), 2.39 (d, $J = 12.6$ Hz, 1H; $CH_2$), 2.37 (m, 4H; [P]$CH_2$), 2.17 (d, $J = 12.6$ Hz, 1H; $CH_2$), 1.65 (m, 4H; [P]$CH_2$), 1.63 (s, 3H; Me), 1.31 (s, 3H; Me), 1.02 (s, 3H; Me); $^{31}P$ NMR (160 MHz, $CD_2Cl_2$, 25 °C): $\delta = 38.72$ (s; P), 38.21 (s; P); $^{13}C$ NMR (150 MHz, $CD_2Cl_2$, 25 °C): $\delta = 157.5$ ($C_6H_3$), 156.2 ($C_6H_4$), 150.8 ($C_6H_3$), 145.0 ($C_6H_3$), 143.2 ($C_6H_4$), 133.6 (m; Ph), 131.8 (m; Ph), 129.5 (d, $J = 11$ Hz; Ph), 127.7 ($C_6H_4$), 123.1 ($C_6H_3$), 115.1 ($C_6H_4$), 113.1 ($C_6H_3$), 112.8 ($C_6H_3$), 97.9 (m, *C*≡CAu), 59.8 ($CH_2$), 57.1 ($OCH_2$), 57.0 ($OCH_2$), 50.4 (*C*Me), 42.4 (*C*$Me_2$), 31.4 (Me), 30.9 (s; 2Me), 27.6(m, [P]$CH_2$), 27.0(m, [P]$CH_2$); elemental analysis calcd (%) for $C_{52}H_{50}Au_2P_2O_2 \cdot 3H_2O$ (1216.9): C 51.33, H 4.64; found: C 51.34, H 4.52.

**Simple ring 11d**: This was prepared similarly from **10** (0.113 g, 0.153 mmol) and $Ph_2P(CH_2)_5PPh_2$ (0.057 g, 0.129 mmol). The product was isolated as a white solid. Yield 0.127 g, 84 %. IR (Nujol): $\tilde{\nu} = 2133$ (w) $cm^{-1}$ (C≡C); $^1H$ NMR (600 MHz, $CD_2Cl_2$, 25 °C): $\delta = 7.66 - 7.40$ (m, 20H; Ph), 7.16 (m, 2H; $C_6H_4$), 7.11 (m, 1H; $C_6H_3$), 6.94 (m, 2H; $C_6H_4$), 6.93 (m, 1H; $C_6H_3$), 6.86 (s br, 1H; $C_6H_3$), 4.81, 4.74 (AB q, $J = 15.6$ Hz, 2H; $OCH_2$), 4.63, 4.52 (AB q, $J = 16.8$ Hz, 2H; $OCH_2$), 2.43 (m, 4H; [P]$CH_2$), 2.37 (d, $J = 12.6$ Hz, 1H; $CH_2$), 2.18 (d, $J = 12.6$ Hz, 1H; $CH_2$), 1.64 (s, 3H; Me), 1.59 (m, 6H; [P]$CH_2$), 1.32 (s, 3H; Me), 1.03 (s, 3H; Me); $^{31}P$ NMR (160 MHz, $CD_2Cl_2$, 25 °C): $\delta = 37.80$ (s; P), 36.97 (s; P); $^{13}C$ NMR (150 MHz, $CD_2Cl_2$, 25 °C): $\delta = 157.5$ ($C_6H_3$), 156.1 ($C_6H_4$), 150.5 ($C_6H_3$), 145.0 ($C_6H_3$), 143.2 ($C_6H_4$), 133.7 (m br; Ph), 131.8 (s br; Ph), 131.7 (m w; *C*≡CAu), 129.4 (d, $J = 10$ Hz; Ph), 127.7 ($C_6H_4$), 123.2 ($C_6H_3$), 114.9 ($C_6H_4$), 113.8 ($C_6H_3$), 112.6 ($C_6H_3$), 97.9 (m, *C*≡CAu), 59.8 ($CH_2$), 57.2 ($OCH_2$), 56.7 ($OCH_2$), 50.5 (*C*Me), 42.5 (*C*$Me_2$), 32.5 (m, [P]$CH_2$), 31.6 (Me), 30.8 (s br; 2Me), 27.8(m, [P]$CH_2$), 25.3(m, [P]$CH_2$); elemental analysis calcd (%) for $C_{53}H_{52}Au_2P_2O_2 \cdot CH_2Cl_2$ (1261.8): C 51.40, H 4.31; found: C 51.19, H 4.24.

**Mixed-phosphane reactions**: All seven pairwise combinations of the diphosphanes $Ph_2P(CH_2)_xPPh_2$ ($x = 2-5$) (0.014 mmol) were treated with oligomer **3** (0.020 g, 0.028 mmol). The mixtures in $CH_2Cl_2$ (20 mL) were stirred for about 3 h to give clear solutions. Activated charcoal was then added to each solution, and the mixtures were filtered. The filtrates were evaporated to dryness under reduced pressure and the residues washed with $Et_2O$ (50 mL) to give white solids. These products were dried and analyzed by $^1H$ and $^{31}P$ NMR spectroscopy.

**X-ray structure determinations**: Data for **4a**, **4d**, and **5a** were collected by using a Nonius Kappa-CCD diffractometer using COLLECT (Nonius, 1998) software. Standard settings were used except for complex **5a**, which has a long axis and required the detector to be moved back to accommodate this. The unit cell parameters were calculated and refined from the full data set. Crystal cell refinement and data reduction was carried out using the Nonius DENZO package. The absorption correction was carried out by integration using SCALEPACK (Nonius, 1998). All crystal data and refinement parameters are listed in Table 6 and Table 7. The SHELXTL 5.1 (Sheldrick, G.M., Madison, WI) program package was used to solve all structures, which were refined using least-squares methods. Data for **4c** were collected by using a Bruker SMART CCD diffractometer. The software used was: SMART, for collecting frames of data, indexing reflection and determination of lattice parameters; SAINT, for integration of intensity of reflections and scaling; SADABS, for absorption correction.

**4a**: A crystal of [{$\mu$-$CMe_2(C_6H_4OCH_2CCAu)_2$}{$\mu$-$Ph_2P(CH_2)_2PPh_2$}] · $0.75\,CH_2Cl_2$ was mounted on a glass fiber. There was disorder in the O(4) through O(20) chain and that unit was modeled as two half-occupancy chains with isotropic thermal parameters. Also, the aromatic rings were restrained to be flat and the C–C distances were constrained to be 1.395 Å. All other non-hydrogen atoms were refined with anisotropic thermal parameters. The hydrogen atoms were calculated geometrically and were riding on their respective carbon atoms. Two molecules of dichloromethane of solvation were found; one was modeled at half occupancy with anisotropic thermal parameters, and hydrogen atoms, the other was modeled (occ = 0.25) isotropically without hydrogen atoms. Both solvent molecules had C–Cl distances fixed to 1.65 Å and Cl–Cl distance fixed to 2.74 Å.

Table 6. Crystal data and structure refinement for complexes **4a** and **4c**.

| Compound | **4a** · $0.75\,CH_2Cl_2$ | **4c** · $0.5\,Et_2O$ |
|---|---|---|
| formula | $C_{47.75}H_{43}Au_2Cl_{1.50}O_2P_2$ | $C_{49}H_{43}Au_2O_{2.50}P_2$ |
| Fw | 1157.87 | 1127.71 |
| $T$ [K] | 292(2) | 293(2) |
| $\lambda$ ($Mo_{K\alpha}$) [Å] | 0.71073 | 0.71073 |
| crystal system | monoclinic | monoclinic |
| space group | $P2(1)/n$ | $P2(1)/n$ |
| $a$ [Å] | 17.9418(7) | 18.0898(7) |
| $b$ [Å] | 14.4752(6) | 14.0949(4) |
| $c$ [Å] | 20.1253(6) | 20.8820(9) |
| $\beta$ [°] | 111.736(2) | 111.875(1) |
| $V$ [Å$^3$] | 4855.1(3) | 4941.0(3) |
| Z | 4 | 4 |
| $\rho_{calcd}$ [mg m$^{-3}$] | 1.584 | 1.516 |
| $\mu$ [mm$^{-1}$] | 6.218 | 6.030 |
| $F$(000) | 2236 | 2180 |
| absorption correction | integration | SADABS |
| measured reflections | 33078 | 22192 |
| unique reflections | 9880 ($R_{int} = 0.1980$) | 8270 ($R_{int} = 0.1398$) |
| parameters | 453 | 277 |
| GOF on $F^2$ | 1.016 | 1.129 |
| $R1$ [$I > 2\sigma(I)$] | 0.0823 | 0.1157 |
| $wR2$ (on $F^2$, all data) | 0.1386 | 0.2363 |
| $\Delta\rho_{min\ and\ max}$ [e Å$^{-3}$] | 0.646 and −0.800 | 2.203 and −0.834 |

Table 7. Crystal data and structure refinement for simple ring **4d** and single braid [2]catenane **5a**.

| Compound | **4d** · $0.4\,Et_2O$ | **5a** · $0.125\,C_2H_4Cl_2$ |
|---|---|---|
| formula | $C_{48.60}H_{44}Au_2O_{2.40}P_2$ | $C_{96.50}H_{89}Au_4Cl_{0.50}O_4P_4$ |
| Fw | 1122.31 | 2242.14 |
| $T$ [K] | 298(2) | 150(2) |
| $\lambda$ ($Mo_{K\alpha}$) [Å] | 0.71073 | 0.71073 |
| crystal system | monoclinic | monoclinic |
| space group | $P2(1)/n$ | $P2(1)/n$ |
| $a$ [Å] | 17.9091(11) | 12.4526(3) |
| $b$ [Å] | 14.1034(10) | 45.0061(18) |
| $c$ [Å] | 21.0868(11) | 30.5379(11) |
| $\beta$ [°] | 114.309(4) | 98.570(2) |
| $V$ [Å$^3$] | 4853.9(5) | 16923.6(10) |
| Z | 4 | 8 |
| $\rho_{calcd}$ [mg m$^{-3}$] | 1.536 | 1.760 |
| $\mu$ [mm$^{-1}$] | 6.138 | 7.056 |
| $F$(000) | 2171 | 8676 |
| absorption correction | integration | integration |
| measured reflections | 31713 | 27409 |
| unique reflections | 6502 ($R_{int} = 0.206$) | 18686 ($R_{int} = 0.0990$) |
| parameters | 450 | 1450 |
| GOF on $F^2$ | 1.067 | 1.059 |
| $R1$ [$I > 2\sigma(I)$] | 0.0793 | 0.0889 |
| $wR2$ (on $F^2$, all data) | 0.1744 | 0.1963 |
| $\Delta\rho_{min\ and\ max}$ [e Å$^{-3}$] | 1.728 and −0.689 | 1.610 and −1.621 |

**4c**: A crystal of [{$\mu$-$CMe_2(C_6H_4OCH_2CCAu)_2$}{$\mu$- $Ph_2PC{\equiv}CPPh_2$}] · $0.5\,Et_2O$ was mounted inside a capillary tube and flame-sealed.

**4d**: A crystal of [{$\mu$-$CMe_2(C_6H_4OCH_2CCAu)_2$}{$\mu$- $Ph_2PC(H)C(H)PPh_2$}] · $0.4\,Et_2O$ was mounted on a glass fiber. All non-hydrogen atoms were refined anisotropically. The hydrogen atoms were calculated geometrically and were riding on their respective atoms. The diethyl ether of solvation

was modeled isotropically at 0.4 occupancy with hydrogen atoms included and some constraints.

**5a**: A crystal of $[\{[\mu\text{-}CMe_2(C_6H_4OCH_2CCAu)_2][\mu\text{-}Ph_2P(CH_2)_3PPh_2]\}_2]\cdot 0.125\,C_2H_4Cl_2$ was mounted on a glass fiber. Most non-hydrogen atoms were refined with anisotropic thermal parameters, but several carbon atoms were isotropic since the quality of the data did not allow anisotropic refinement. The $Me_2C$ unit was modeled in the case of the A molecule as two separate units each with half occupancy. The hydrogen atoms were calculated as described above.

Crystallographic data (excluding structure parameters) for the structures reported in this paper have been deposited with the Cambridge Crystallographic Data Centre as supplementary publication nos. CCDC 120855 (**4a**), CCDC 170368 (**4c**), CCDC 170369 (**4d**), and CCDC 120856 (**5a**). Copies of the data can be obtained free of charge on application to CCDC, 12 Union Road, Cambridge CB2 1EZ, UK (fax: (+44) 1223 336–033; e-mail: deposit@ccdc.cam.ac.uk).

## Acknowledgements

We thank Dr. C. Kirby (UWO) for assistance with NMR experiments and the NSERC (Canada) for financial support. R.J.P. thanks the Government of Canada for a Canada Research Chair.

[1] For recent reviews see: a) *Molecular Catenanes, Rotaxanes and Knots* (Eds.: J.-P. Sauvage, C. O. Dietrich-Buchecker), Wiley-VCH, Weinheim, **1999**; b) M. Fujita, *Acc. Chem. Res.* **1999**, *32*, 53–61; c) F. M. Raymo, J. F. Stoddart, *Chem. Rev.* **1999**, *99*, 1643–1663; d) S. Leininger, B. Olenyuk, P. J. Stang, *Chem. Rev.* **2000**, *100*, 853–908; e) S. R. Batten, R. Robson, *Angew. Chem.* **1998**, *110*, 1558–1595; *Angew. Chem. Int. Ed.* **1998**, *37*, 1460–1494; f) G. F. Swiegers, T. J. Malefetse, *Chem. Rev.* **2000**, *100*, 3483–3537; g) F. Vögtle, T. Dünnwald, T. Schmidt, *Acc. Chem. Res.* **1996**, *29*, 451–460; g) A. R. Pease, J. O. Jeppeson, J. F. Stoddart, Y. Luo, C. P. Collier, J. R. Heath, *Acc. Chem. Res.* **2001**, *34*, 433.

[2] For recent examples see: a) C. Reuter, W. Wienand, C. Schmuck, F. Vögtle, *Chem. Eur. J.* **2001**, *7*, 1728–1733; b) O. Safarowsky, M. Nieger, R. Fröhlich, F. Vögtle, *Angew. Chem.* **2000**, *112*, 1699–1701; *Angew. Chem. Int. Ed.* **2000**, *39*, 1616–1618; c) M. Consuelo Jimenez, C. Dietrich-Buchecker, J.-P. Sauvage, A. De Cian, *Angew. Chem.* **2000**, *112*, 1351–1354; *Angew. Chem. Int. Ed.* **2000**, *39*, 1295–1298; d) M. Fujita, N. Fujita, K. Ogura, K. Yamaguchi, *Nature* **1999**, *400*, 52–55; e) S.-G. Roh, K.-M. Park, G.-J. Park, S. Sakamoto, K. Yamaguchi, K. Kim, *Angew. Chem.* **1999**, *111*, 672–675; *Angew. Chem. Int. Ed.* **1999**, *38*, 638–640; f) Q. Zhang, D. G. Hamilton, N. Feeder, S. J. Teat, J. M. Goodman, J. K. M. Sanders, *New J. Chem.* **1999**, *23*, 897–903; g) B. Cabezon, J. Cao, F. M. Raymo, J. F. Stoddart, A. J. P. White, D. J. Williams, *Angew. Chem.* **2000**, *112*, 152–155; *Angew. Chem. Int. Ed.* **2000**, *39*, 148–151.

[3] For recent nanotechnology applications see: a) J.-P. Sauvage, *Science* **2001**, *291*, 2105–2106; b) P. R. Ashton, R. Ballardini, V. Balzani, A. Credi, K. R. Dress, E. Ishow, C. J. Kleverlaan, O. Kocian, J. A. Preece, N. Spencer, J. F. Stoddart, M. Venturi, S. Wenger, *Chem. Eur. J.* **2000**, *6*, 3558–3574; c) C. P. Collier, G. Mattersteig, E. W. Wong, Y. Luo, K. Beverly, J. Sampaio, F. M. Raymo, J. F. Stoddart, J. R. Heath, *Science* **2000**, *289*, 1172–1175; d) V. Balzani, A. Credi, F. M. Raymo, J. F. Stoddart, *Angew. Chem.* **2000**, *112*, 3484–3530; *Angew. Chem. Int. Ed.* **2000**, *39*, 3348–3391; e) C. P. Collier, E. W. Wong, M. Belohradsky, F. M. Raymo, J. F. Stoddart, P. J. Kuekes, R. S. Williams, J. R. Heath, *Science* **1999**, *285*, 391–394; f) M. J. Blanco, M. C. Jimenez, J. C. Chambron, V. Heitz, M. Linke, J.-P. Sauvage, *Chem. Soc. Rev.* **1999**, *28*, 293–305.

[4] a) E. Wasserman, *J. Am. Chem. Soc.* **1960**, *82*, 4433–4434; b) H. L. Frisch, E. Wasserman, *J. Am. Chem. Soc.* **1961**, *83*, 3789–3795; c) G. Schill, *Catenanes, Rotaxanes and Knots*, Academic Press, New York, **1971**; d) D. M. Walba, *Tetrahedron* **1985**, *41*, 3161–3212.

[5] A further example of an organometallic catenane has been reported recently: M. R. Wiseman, P. A. Marsh, P. T. Bishop, B. J. Brisdon, M. F. Mahon, *J. Am. Chem. Soc.* **2000**, *122*, 12598–12599.

[6] G.-J. M. Gruter, F. J. J. de Kanter, P. R. Markies, T. Nomoto, O. S. Akkerman, F. Bickelhaupt, *J. Am. Chem. Soc.* **1993**, *115*, 12179–12180.

[7] D. M. P. Mingos, J. Yau, S. Menzer, D. J. Williams, *Angew. Chem.* **1995**, *107*, 2045–2047; *Angew. Chem. Int. Ed. Engl.* **1995**, *34*, 1894–1895.

[8] a) W. J. Hunks, M. C. Jennings, R. J. Puddephatt, *Inorg. Chem.* **1999**, *38*, 5930–5932; b) R. J. Puddephatt, *Chem. Commun.* **1998**, 1055–1062; c) M. J. Irwin, J. J. Vittal, R. J. Puddephatt, *Organometallics* **1997**, *16*, 3541–3547; d) M. J. Irwin, L. Manojlovic Muir, K. W. Muir, R. J. Puddephatt, D. S. Yufit, *Chem. Commun.* **1997**, 219–220; e) R. J. Puddephatt, *Coord. Chem. Rev.* **2001**, *216–217*, 313–332.

[9] For examples see: a) A. Hirsch, M. Hanack in *Conjugated Polymeric Materials: Opportunities in Electronics, Optoelectronics and Molecular Electronics* (Eds.: J. L. Bredas, R. R. Chance), Kluwer, New York, **1990**, 163; b) M. Hanack, A. Datz, R. Fay, K. Fischer, U. Kepeler, J. Koch in *Handbook of Conducting Polymers* (Ed.: T. A. Skotheim), Marcel Dekker, New York, **1986**, 117.

[10] A. Grohmann, H. Schmidbaur in *Comprehensive Organometallics II* (Eds.: E. Abel, F. G. A. Stone, G. Wilkinson), Elsevier, Oxford, **1995**, *Vol. 3*, 1–56.

[11] a) H. Schmidbaur, A. Grohmann, M. E. Olmos in *Gold: Progress in Chemistry, Biochemistry and Technology* (Ed.: H. Schmidbaur), Wiley, Chichester, **1999**, Ch. 18; b) P. Pyykkö, *Chem. Rev.* **1997**, *97*, 597–636.

[12] C. P. McArdle, M. J. Irwin, M. C. Jennings, R. J. Puddephatt, *Angew. Chem.* **1999**, *111*, 3571–3573; *Angew. Chem. Int. Ed.* **1999**, *38*, 3376–3378.

[13] C. P. McArdle, J. J. Vittal, R. J. Puddephatt, *Angew. Chem.* **2000**, *112*, 3977–3980; *Angew. Chem. Int. Ed. Engl.* **2000**, *39*, 3819–3822.

[14] M. S. Deleuze, D. A. Leigh, F. Zerbetto, *J. Am. Chem. Soc.* **1999**, *121*, 2364–2379.

[15] C. P. McArdle, M. C. Jennings, J. J. Vittal, R. J. Puddephatt, *Chem. Eur. J.* **2001**, *7*, 3572–3583.

[16] a) I. Dance, M, Scudder, *Chem. Eur. J.* **1996**, *2*, 481–486; b) C. A. Hunter, *Chem. Soc. Rev.* **1994**, 101–109; c) C. A. Hunter, J. K. M. Sanders, *J. Am. Chem. Soc.* **1990**, *112*, 5525–5534.

[17] C. A. Hunter, *J. Am. Chem. Soc.* **1992**, *114*, 5303–5311.

[18] a) J. M. Forward, J. P. Fackler Jr., Z. Assefa in *Optoelectronic Properties of Inorganic Compounds* (Eds.: M. D. Roundhill, J. P. Fackler Jr.), Plenum Press, New York, **1999**, 195–239; b) V. W. W. Yam, K. K. W. Lo, *Chem. Soc. Rev.* **1999**, *28*, 323–334; c) W. J. Hunks, M.-A. MacDonald, M. C. Jennings, R. J. Puddephatt, *Organometallics* **2000**, *19*, 5063–5070.

[19] a) M. Fujita, F. Ibukuro, K. Yamaguchi, K. Ogura, *J. Am. Chem. Soc.* **1995**, *117*, 4175; b) Y. Yamanoi, Y. Sakamoto, T. Kusukawa, M. Fujita, S. Sakamoto, K. Yamaguchi, *J. Am. Chem. Soc.* **2001**, *123*, 980–981.

[20] For examples of chiral catenanes see: a) D. K. Mitchell, J.-P. Sauvage, *Angew. Chem.* **1988**, *100*, 985–985; *Angew. Chem. Int. Ed. Engl.* **1988**, *27*, 930–931; b) J.-C. Chambron, D. K. Mitchell, J.-P. Sauvage, *J. Am. Chem. Soc.* **1992**, *114*, 4625–4631; c) C. Yamamoto, Y. Okamoto, T. Schimdt, R. Jäger, F. Vögtle, *J. Am. Chem. Soc.* **1997**, *119*, 10547–10548; d) P. R. Ashton, A. M. Heiss, D. Pasini, F. M. Raymo, A. N. Shipway, J. F. Stoddart, N. Spencer, *Eur. J. Org. Chem.* **1999**, 995–1004.

[21] A. Tamaki, J. K. Kochi, *J. Organomet. Chem.* **1974**, *64*, 411–425.

Received: September 20, 2001 [F3564]

  